AIP | Applied Physics Letters

Size effects on thermoelectric behavior of ultrathin Na x CoO2 films

Peter Brinks, Guus Rijnders, and Mark Huijben

Citation: Applied Physics Letters **105**, 193902 (2014); doi: 10.1063/1.4901447
View online: http://dx.doi.org/10.1063/1.4901447
View Table of Contents: http://scitation.aip.org/content/aip/journal/apl/105/19?ver=pdfcov
Published by the AIP Publishing

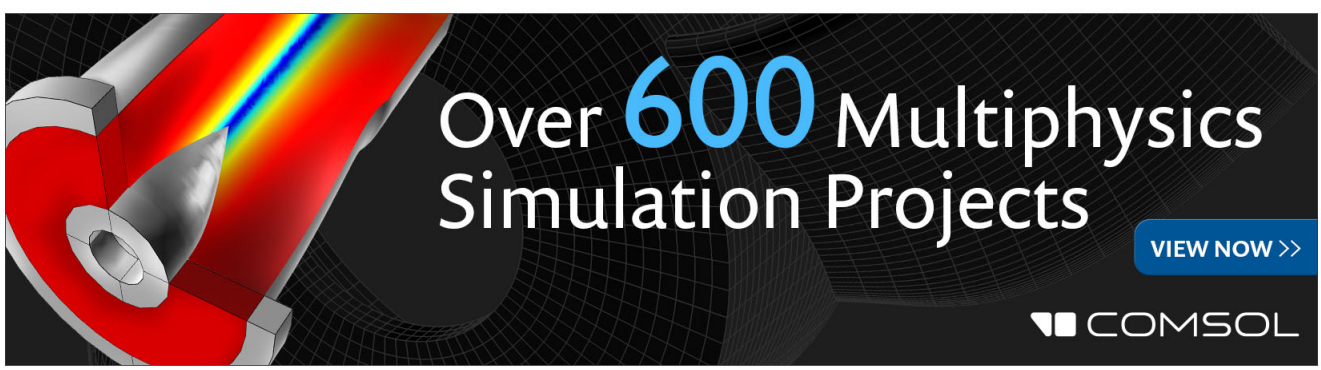

Size effects on thermoelectric behavior of ultrathin Na_xCoO_2 films

Peter Brinks, Guus Rijnders, and Mark Huijben[a)]
Faculty of Science and Technology and MESA+ Institute for Nanotechnology, University of Twente, P.O. Box 217, 7500 AE, Enschede, The Netherlands

(Received 2 October 2014; accepted 30 October 2014; published online 10 November 2014)

Size effects in thermoelectric Na_xCoO_2 thin films are studied, focusing on the electrical resisitivity and Seebeck coefficient. For very thin films below 10 nm, we have observed an increase in resistivity, which is in agreement with theoretical models. In contrast to a predicted simultaneous suppression of the Seebeck coefficient for ultrathin films, we observe a constant Seebeck coefficient as a function of layer thickness due to changes in the structural properties as well as the presence of strong electron correlations. This preserved high Seebeck coefficient opens up new directions for Na_xCoO_2 ultrathin films as basic building blocks in thermoelectric superlattices with enhanced phonon scattering. © *2014 AIP Publishing LLC*. [http://dx.doi.org/10.1063/1.4901447]

Thermoelectric energy conversion is currently gaining interest because of the potential to convert waste heat into electrical energy. However, the search for new and improved materials remains the key factor for enhancement of the overall efficiency of this conversion process. Engineering of improved thermoelectric materials is challenging because of the direct interplay between the relevant material properties. To improve the overall thermoelectric performance of a material, the electrical conductivity and Seebeck coefficient have to be increased, whereas the thermal conductivity should simultaneously be suppressed. Among a wide variety of thermoelectric materials, oxides are studied as promising candidate materials because of their good thermal and chemical stability, making them ideal for high-temperature applications.[1,2] Within the class of oxide materials, the layered cobaltates, such as Na_xCoO_2, have been shown to give excellent thermoelectric properties[2] with dimensionless figure of merit (ZT values) up to ~1.2 at 800 K for Na_xCoO_2 single crystals.[3]

For the successful application of cobaltates in thermoelectric energy generators further improvement of the thermoelectric properties is required. The development into thin films offers an alternative approach to improve the specific thermoelectric properties, because of enhanced phonon scattering at the interfaces. By limiting the phonon transport in ultrathin films the thermal conductivity can be significantly suppressed, as reported previously for other material systems,[4,5] and has led to dramatic improvements of the thermoelectric properties of telluride superlattices.[6,7] However, because of enhanced surface scattering in such ultrathin films, a decrease in electrical conductivity and Seebeck coefficient is expected, based on, respectively, Tellier's[8] and Pichard's[9] model. This reduction in electronic properties is originating from the structural properties of the ultrathin films, as the scattering is determined by the defect density. Control over the structural quality in these ultrathin cobaltate films is imperative to establish optimized electrical conductivity as well as Seebeck coefficient, in contradiction to theoretical predictions.[8,9]

In this work, we study the size effect dependence on the thermoelectric performance of ultrathin Na_xCoO_2 films, in which thin films with reduced thicknesses down to 5 nm are grown on single crystal substrates. Previously it was shown that structural engineering in Na_xCoO_2 films led to enhanced thermoelectric properties when grown on $(LaAlO_3)_{0.3}(Sr_2AlTaO_6)_{0.7}$ (LSAT) and $LaAlO_3$ single crystal substrates.[10] Here, we show that Na_xCoO_2 thin films with thicknesses below 60 nm exhibit an increase in resistivity, which is in agreement with theoretical modeling.[8] Most interestingly, the theoretically predicted decrease of the Seebeck coefficient[9] remains absent as ultrathin Na_xCoO_2 films down to 10 nm show preservation of high Seebeck values. This control of the structural quality in ultrathin Na_xCoO_2 films makes these cobaltate thin films promising candidates as building blocks in thermoelectric superlattices for further development into thermoelectric energy convertors.

Thin films of Na_xCoO_2 were deposited by Pulsed Laser Deposition (PLD) on single crystal $LaAlO_3$ (001) and LSAT (001) substrates (Crystec GmbH). The $LaAlO_3$ and LSAT substrates were annealed, respectively, at 950 °C for 1 h and at 1050 °C for 10 h in an oxygen flow of 150 ml/min to exhibit smooth surfaces with clear unit-cell-height steps in atomic force microscopy (AFM).[10] The thin films were deposited in an oxygen background pressure of 0.4 mbar and at a substrate temperature of 430 °C, while a sintered $Na_{0.9}CoO_2$ target was ablated with a laser fluence of 4 J/cm^2 and at a repetition rate of 1 Hz. After growth, the thin films were slowly cooled to room temperature in 1 bar of oxygen at a rate of 10 °C/min to optimize the oxidation level. In order to maintain the chemical stability of the thin films, an amorphous AlO_x capping layer was deposited *in situ* on top of the Na_xCoO_2 thin films.[11] The thin films were characterized by X-Ray diffraction (XRD Bruker D8 and Panalytical XPert Pro MRD) and AFM (Bruker Dimension Icon) to obtain detailed information about, respectively, crystallinity and surface morphology. Electrical conductivity was measured using a Physical Properties Measurement System (PPMS, Quantum Design), while Seebeck measurements were performed using a custom built Seebeck measurement setup, verified with a NIST standard reference sample.[12]

To study the size effects on the thermoelectric performance of Na_xCoO_2 thin films, the dependence of thin film thickness, between 5 and 250 nm, was determined on the structural and thermoelectric properties. In order to verify the correct

[a)]Electronic mail: m.huijben@utwente.nl

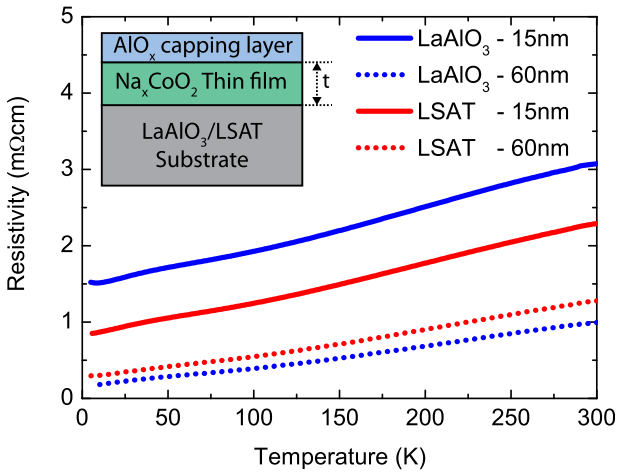

FIG. 1. The temperature dependent resistivity for Na_xCoO_2 thin films with varying thickness t deposited on $LaAlO_3$ (001) and LSAT (001) single crystal substrates.

thermoelectric phase exhibiting metallic behavior, the resistivity as a function of temperature is shown in Fig. 1. A clear metallic behavior can be observed for thin films with a strongly reduced layer thickness of ~15 nm similar to previously reported thin films[10] with thicknesses of ~60 nm, indicating controlled electrical properties with preservation of the overall transport behavior irrespective of layer thickness and substrate material. This is supported by Hall measurements (not shown), which demonstrate a constant carrier density of $1–2 \times 10^{21}\,cm^{-3}$, calculated by a simple single band model, for all thin films at room temperature in combination with a constant carrier mobility of $1–2\,cm^2V^{-1}s^{-1}$ in good agreement with previous reports.[10,11] However, for the full detailed analysis of the temperature dependent transport behavior[10] a more extensive t-J model is required taking into account the strong electron correlations in Na_xCoO_2 as well as the two-dimensional nature of the triangular CoO_2 layers.[13,14]

The presence of a single-phase Na_xCoO_2 thin film, and absence of impurity phases, is confirmed by XRD, which only shows (00l) Na_xCoO_2 peaks for $2\theta/\omega$ scans between 10° and 110°, indicating oriented growth with the c-axis perpendicular to the surface of the thin films. Detailed reciprocal space maps (RSMs) around the (002) Na_xCoO_2 diffraction peak are shown in Fig. 2 for thin films with varying thicknesses on both $LaAlO_3$ as well as LSAT substrates. Clear structural differences are observed for thin films with varying layer thicknesses on each type of substrate. For very thin films, a sharp line is observed in the $2\theta/\omega$ direction, with only a very limited width in the ω direction, which represents a highly crystalline phase with a very well defined orientation (tilt). The observed width in $2\theta/\omega$ direction is a direct consequence of the finite thickness of the thin films. The presence of multiple peaks (sharp lines) for thin films on $LaAlO_3$ substrates is a direct consequence of the various crystallographic domains in the substrate crystal. For increased layer thicknesses, a second peak with a significantly larger width in the ω direction is appearing. This is caused by an increasing variation of tilt angles of the unit cell for increased layer thicknesses and is known to occur by the formation of misfit dislocations in thin films with a relatively large lattice mismatch with respect to their substrate, as previously predicted and observed for other material systems[15,16] as well as for Na_xCoO_2 thin films.[10]

The RSMs indicate that these two different diffraction peaks (sharp and diffuse) are positioned at equal 2θ values, indicating that the two peaks are originating from crystalline parts with the same lattice constant but a small tilt angle with respect to each other. The c-axis lattice parameter in Na_xCoO_2 is previously reported to vary with the composition[17–21] and the observed value suggests a constant composition of $Na_{0.67}CoO_2$ for all thin films,[10,17] irrespective of the layer thickness. The formation of misfit dislocations depends on the choice of substrate material and thin film layer thickness. The critical thickness at which such misfit dislocations start to form is dependent on the lattice mismatch between the substrate and thin film.[22–24] However, in this case, the difference in crystal symmetry between substrate and Na_xCoO_2 thin film has to be taken into account as well in addition to the difference in lattice parameter. From the RSMs, it is concluded that the critical thickness for the onset of misfit dislocations is around 10 nm for these thin films.

To study the structural properties in more detail, $2\theta/\omega$ scans and ω scans (rocking curves) of these thin films are shown in Fig. 3. In the rocking curves, the presence of a diffuse and a sharp peak is confirmed and the ratio of the two different contributions can be clearly observed. It is seen that the diffuse peak is increasing rapidly and is becoming more significant with increasing thickness. This is especially clear for the samples on LSAT, where the sharp peak can no longer be observed for a thickness of 100 and 250 nm. This is a direct consequence of the increasing amount of volume of the sample which has a less defined orientation (tilt). Overall, it is clear that the samples on $LaAlO_3$ are more crystalline, which can be best observed by comparing the thin films with a thickness of 10 nm. For the sample on $LaAlO_3$, the peak is significantly more pronounced than for the sample on LSAT in the $2\theta/\omega$ as well as the rocking curve scans.

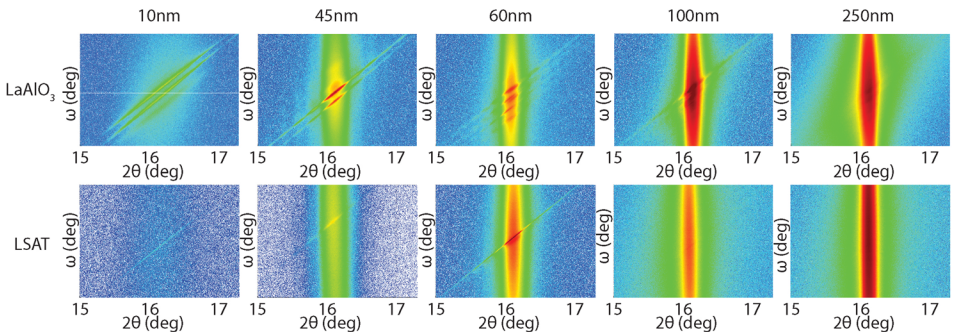

FIG. 2. XRD RSMs for Na_xCoO_2 thin films with varying layer thickness deposited on $LaAlO_3$ (top) and LSAT (bottom) single crystal substrates. Scans are made around the (002) Na_xCoO_2 diffraction peak. Color scale is logarithmic and equal for each type of substrate to enable comparison of the intensity distributions.

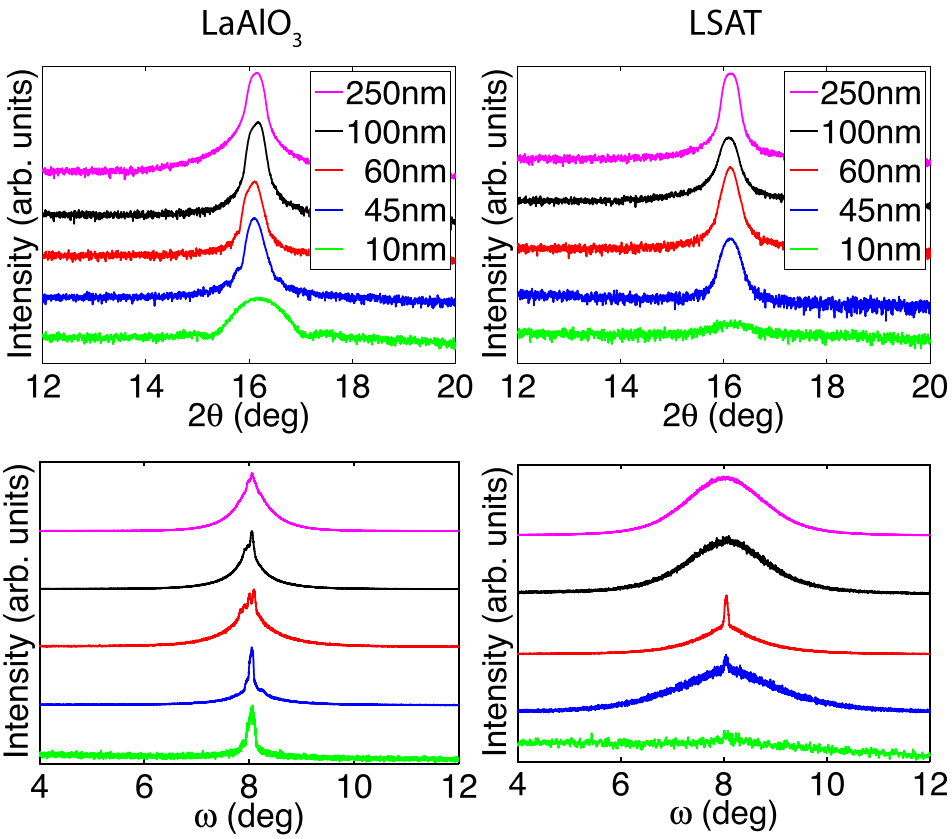

FIG. 3. XRD analysis by $2\theta/\omega$ scans (top) and ω scans (bottom) around the (002) diffraction peak of Na_xCoO_2 thin films with varying layer thickness deposited on $LaAlO_3$ (left) and LSAT (right) single crystal substrates. The scans are vertically shifted for clarity.

Even though the crystallinity is reduced for the samples deposited on LSAT, it can be concluded that for very thin layers below the critical thickness, the layers have a significantly lower orientational spread.

Based on theoretical predictions, it is expected that by reducing the layer thickness of metallic thin films, surface scattering is enhanced, leading to a strong increase of the resistivity. Additionally, the Seebeck coefficient is expected to decrease for very thin layers. For both the resistivity ρ_f as well as the Seebeck coefficient S_f, an inverse thickness dependence is expected based on Tellier's[8] and Pichard's[9] models

$$\rho_f(t) = \rho_b\left(1 + \frac{3l_b}{8t}(1-p)\right), \tag{1}$$

$$S_f(t) = S_b\left(1 - \frac{3l_b}{8t}(1-p)\frac{U_b}{1+U_b}\right), \tag{2}$$

where ρ_b is the bulk resistivity, S_b is the bulk Seebeck coefficient, l_b is the bulk electron mean free path, p is the specularity parameter, U_b is the energy-dependent scattering term, and t is the layer thickness. The appearance of this size effect is mainly dependent on the electron mean free path, which determines the thickness at which the resistivity starts to increase and the specularity parameter, p, which determines the strength of the effect. The value of p is a measure of the atomic order (crystallinity) of the thin films, which limits are zero for fully disordered polycrystalline thin films and 1 for perfect single crystalline epitaxial thin films. In the latter case, no size effect can be observed.

The room temperature resistivity of Na_xCoO_2 thin films deposited on $LaAlO_3$ and LSAT substrates as a function of layer thickness is shown in Fig. 4. It can be clearly observed that the resistivity increases when the film thickness is reduced, as expected from Tellier's model. To obtain a good fit, the value of the bulk resistivity ρ_b is determined by averaging values for films above a thickness of 60 nm, while the value of l_b is determined from the slope of the resistivity versus 1/t and assuming the ideal case with p-value of zero. With these values of l_b and ρ_b, the complete data set were fitted to obtain the specularity parameter p. The resulting fits for the thin films on $LaAlO_3$ and LSAT are very comparable and the fit for the thin films on LSAT is shown in Fig. 4. The value obtained for the electron mean free path, l_b, of the fit is 56 nm, which is much larger than values calculated from the room temperature Hall measurements, which lead to an electron mean free path of only 0.7 nm based on a single band model with an effective electron mass of $5\,m_e$ (Ref. 25) and

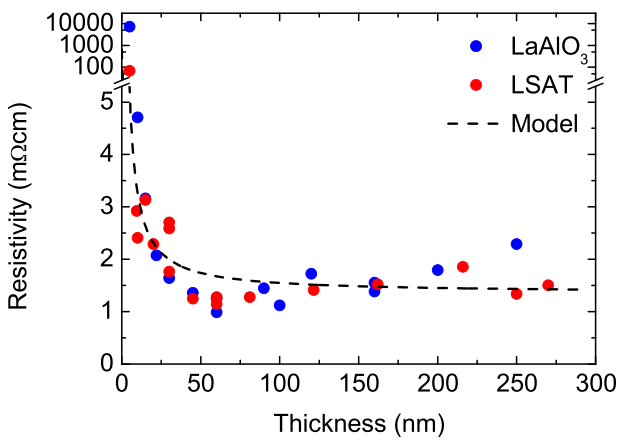

FIG. 4. Resistivity at 300 K as a function of Na_xCoO_2 layer thickness for thin films deposited on $LaAlO_3$ and LSAT single crystal substrates. Measurement errors remain within the symbol size. Dashed line is a fit based on Tellier's model.

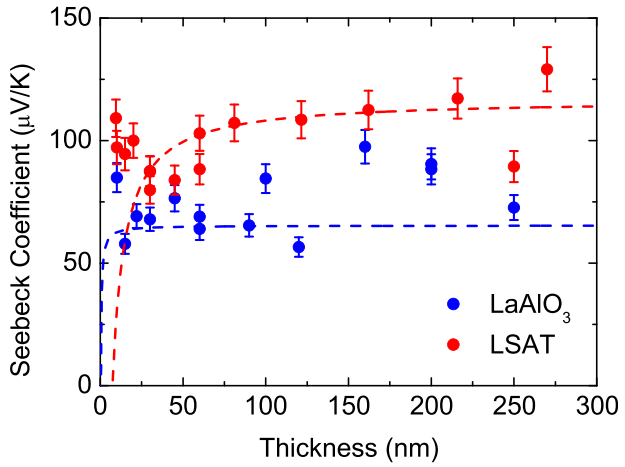

FIG. 5. Seebeck coefficient at 300 K as a function of Na_xCoO_2 layer thickness for thin films deposited on $LaAlO_3$ and LSAT single crystal substrates. Dashed lines are fits based on Pichard's model.

assuming no electron correlations. However, comparable values were obtained for $Bi_2Sr_2Co_2O_y$ thin films[26] and even larger values were reported for thermoelectric tellurides.[27,28] It should however be taken into account that our Na_xCoO_2 thin films remain metallic down to low temperatures, in contrast to $Bi_2Sr_2Co_2O_y$ and the tellurides. Using the obtained ρ_b and l_b values, the best fit is obtained for a specularity parameter, p, of 0.3, which is in good agreement with previous observations that these thin films on LSAT show a high degree of ordering for both out-of-plane and in-plane orientations.[10] From the fits of the thickness dependent resistivity it can be concluded that electron correlations play an important role and have to be taken into account when studying cobaltate thin films.[13,14,26]

The Seebeck coefficient for Na_xCoO_2 thin films deposited on $LaAlO_3$ and LSAT substrates with varying layer thickness is shown in Fig. 5. For both type of substrates fits to Pichard's model of the thickness dependent Seebeck coefficient is shown, based on the results of the fits for the corresponding resistivity data. The bulk Seebeck value S_b is determined by averaging values for films above a thickness of 60 nm. By fitting to Pichard's model the combined values for the bulk Seebeck coefficient and the initial resistivity fits, the energy dependent scattering term U_b can be determined. For thin films deposited on LSAT substrates, a reasonable fit provides a value for U_b of ~1, which is much larger than that observed for Bi_2Te_3-based samples.[27] For ultrathin films down to a thickness of 10 nm a constant Seebeck coefficient of $\sim 100\,\mu V\,K^{-1}$ is measured, in strong contrast to the predicted downturn in Seebeck coefficient according to the simple Pichard's model. Qualitatively comparable behavior is observed for thin films deposited on $LaAlO_3$ substrates. This behavior can be understood by realizing that the structural properties for very thin films are not comparable to thin films with a larger thickness. The increase of orientational spread in these thin films above the critical thickness lead to an enhanced carrier scattering, which is not taken into account by Tellier's and Pichard's models, in which structurally comparable films are assumed, and are causing an additional increase of the resistivity for these thin films above the critical thickness. Furthermore, for very thin films the expected decrease of the Seebeck coefficient is not observed, because of the strong electron correlations. In such strongly correlated materials, the Seebeck coefficient is not dependent on the scattering mechanism.[26] These observations demonstrate again the importance of electron correlations in cobaltate thin films and show Na_xCoO_2 as a promising thermoelectric material, because of the preserved high Seebeck coefficient in ultrathin films. However, the observed increase in resistivity leads to a reduction of the thermoelectric power factor. This could be compensated by a reduced thermal conductivity to preserve the high thermoelectric performance in ultrathin films.

In conclusion, we have observed an increasing resistivity for metallic Na_xCoO_2 thin films, deposited on $LaAlO_3$ as well as LSAT substrates, with a thickness lower than 60 nm, which is in accordance with theoretical predictions. However, the Seebeck coefficient for these thin films remains constant, irrespective of layer thickness, which is a signature of the strong electron correlations in Na_xCoO_2. This separate control over the resistivity and Seebeck coefficient is very promising for Na_xCoO_2 as a thermoelectric material, because the observed high Seebeck coefficient for ultrathin films enables new directions such as building blocks in thermoelectric superlattices with enhanced phonon scattering.

[1]J. R. Sootsman, D. Y. Chung, and M. G. Kanatzidis, Angew. Chem. Int. Ed. **48**, 8616 (2009).
[2]J. He, Y. Liu, and R. Funahashi, J. Mater. Res. **26**, 1762 (2011).
[3]K. Fujita, T. Mochida, and K. Nakamura, Jpn. J. Appl. Phys., Part 1 **40**, 4644 (2001).
[4]M. S. Aubain and P. R. Bandaru, J. Appl. Phys. **110**, 084313 (2011).
[5]M. Maldovan, J. Appl. Phys. **110**, 034308 (2011).
[6]R. Venkatasubramanian, Phys. Rev. B **61**, 3091 (2000).
[7]R. Venkatasubramanian, E. Siivola, T. Colpitts, and B. O'Quinn, Nature **413**, 597 (2001).
[8]C. R. Tellier, Thin Solid Films **51**, 311 (1978).
[9]C. R. Pichard, C. R. Tellier, and A. J. Tosser, J. Phys. F: Met. Phys. **10**, 2009 (1980).
[10]P. Brinks, B. Kuiper, E. Breckenfeld, G. Koster, L. W. Martin, G. Rijnders, and M. Huijben, Adv. Energy Mater. **4**, 1301927 (2014).
[11]P. Brinks, H. Heijmerikx, T. A. Hendriks, G. Rijnders, and M. Huijben, RSC Adv. **2**, 6023 (2012).
[12]N. D. Lowhorn, W. Wong-Ng, Z. Q. Lu, E. Thomas, M. Otani, M. Green, N. Dilley, J. Sharp, and T. N. Tran, Appl. Phys. A **96**, 511 (2009).
[13]W. Koshibae, A. Oguri, and S. Maekawa, Phys. Rev. B **75**, 205115 (2007).
[14]B. S. Shastry, Rep. Prog. Phys. **72**, 016501 (2009).
[15]J. W. Matthews and A. E. Blakeslee, J. Cryst. Growth **27**, 118 (1974).
[16]V. M. Kaganer, R. Köhler, M. Schmidbauer, R. Opitz, and B. Jenichen, Phys. Rev. B **55**, 1793 (1997).
[17]Q. Huang, M. L. Foo, R. A. Pascal, J. W. Lynn, B. H. Toby, T. He, H. W. Zandbergen, and R. J. Cava, Phys. Rev. B **70**, 184110 (2004).
[18]Y. Krockenberger, I. Fritsch, G. Christiani, H. U. Habermeier, L. Yu, C. Bernhard, B. Keimer, and L. Alff, Appl. Phys. Lett. **88**, 162501 (2006).
[19]L. Viciu, J. W. G. Bos, H. W. Zandbergen, Q. Huang, M. L. Foo, S. Ishiwata, A. P. Ramirez, M. Lee, N. P. Ong, and R. J. Cava, Phys. Rev. B **73**, 174104 (2006).
[20]R. Berthelot, D. Carlier, and C. Delmas, Nat. Mater. **10**, 74 (2011).
[21]X. P. Zhang, Y. S. Xiao, H. Zhou, B. T. Xie, C. X. Yang, and Y. G. Zhao, Mater. Sci. Forum **3807**, 475 (2005).
[22]S. M. Hu, J. Appl. Phys. **69**, 7901 (1991).
[23]A. Braun, K. M. Briggs, and P. Böni, J. Cryst. Growth **241**, 231 (2002).
[24]D. C. Houghton, C. J. Gibbings, C. G. Tuppen, M. H. Lyons, and M. A. G. Halliwell, Appl. Phys. Lett. **56**, 460 (1990).
[25]S. Lupi, M. Ortolani, and P. Calvani, Phys. Rev. B **69**, 180506 (2004).
[26]J. Ravichandran, A. K. Yadav, W. Siemons, M. A. McGuire, V. Wu, A. Vailionis, A. Majumdar, and R. Ramesh, Phys. Rev. B **85**, 085112 (2012).
[27]K.-W. Cho and I.-H. Kim, Mater. Lett. **59**, 966 (2005).
[28]Z. Zeng, P. Yang, and Z. Hu, Appl. Surf. Sci. **268**, 472 (2013).